PAPER E

REFLECTION AND TRANSMISSION COEFFICIENTS IN POROUS MEDIA

Xiaofei Chen ** and Youli Quan *

ABSTRACT

In this study we derive a set of exact formulas for the reflection and transmission coefficients in porous media. These formulas directly relate the amplitude of reflected waves to porous parameters, such as porosity, permeability and viscosity. If we can directly estimate porous parameters by performing AVO analysis, it is helpful for reservoir characterization and description. This work provides an effective tool for AVO in porous media. In the conventional AVO analysis, the reflection coefficient is based on *effective* velocity of a porous medium. As numerical tests, we compare the reflection coefficient calculated from our exact formulas with that using the effective velocity for different porous medium models. We find that at low frequency range two results agree very well, but at high frequency range, the solution using the effective velocity departs from the exact solution. We also assess the possible influence of the BISQ model newly developed by Dvorkin and Nur (1993) on AVO analysis. Since the BISQ model gives rise to notably smaller phase velocities at low frequency, thus it will give notably different reflection coefficients. Consequently, it will be significantly affect the results of AVO analysis.

* STP, Stanford University
** Department of Earth Sciences, University of Southern California

INTRODUCTION

AVO analysis of seismic reflection data is widely used to infer the presence of hydrocarbons. The conventional AVO analysis is based on such a strategy: first, one estimates the *effective* elastic parameters of a hydrocarbon reservoir using *elastic* reflection coefficient formulation; then models the reservoir as porous media and infers the porous parameters from those effective elastic parameters. Strictly speaking, this is an approximate approach to the reflection coefficient in porous media. The exact method should be based on the rigorous solutions in porous media. In this study we shall derive such an exact solution for the reflection and transmission coefficients in porous media. With these exact formulas, we can evaluate the validity and accuracy of the approximate method. Since our formulas give a direct relationship between the reflection coefficient and the porous property, we may use this relationship converting the reflection coefficient to porosity and other porous parameters under certain conditions.

This study is also a pilot work for simulation of complete wave fields in porous media. From this study we can understand how we properly propose the boundary conditions in porous media and when an exact porous solution is necessary. The modeling for vertically and/or radially layered porous media is in progress.

MODELS OF POROUS MEDIA

Biot theory (Biot, 1956a,b; 1962a,b) is the bedrock for studying the wave phenomena in porous media. Recently, Dvorkin and Nur (1993) proposed a unified model with squirt and Biot mechanisms (i.e., BISQ model). As shown by Dvorkin and Nur that at low frequency BISQ behaves differently from Biot model, at high frequency it approaches to Biot model. Figure 1 shows comparisons of the fast P-wave for these two porous medium models in the frequency range from 1 Hz to 10^{10}Hz. Here, the density of solid material is ρ_s=2.6284 g/cm^3, density of pore fluid ρ_f=1.0 g/cm^3, additional coupling density ρ_a=0.42g/cm^3, P- wave and S-wave velocities of solid material α_s =5.4497 km/s and β_s=3.2438 km/s, porosity ϕ=0.19, intrinsic permeability κ=100md and viscosity of the pore fluid η=1.0 cp. Note that the Biot's critical frequency for this case is $f_c = \dfrac{\phi\eta}{2\pi\kappa\rho_f} \approx 3\times10^5$Hz, we can clearly see that at low-frequency limit ($f \ll f_c$) the phase velocities of BISQ model have a smaller values than those of Biot model. At high-frequency case ($f > f_c$), however, the velocities for Biot and BISQ models tend to same value.

R/T COEFFICIENTS IN POROUS MEDIA

Let us consider two porous media wedded by a plane permeable interface. According to the acoustic theory of porous media, there are three kinds of waves in each porous medium, i.e., fast and slow P waves, and S wave. Owing to reflection and transmission effect of the interface, we have total six independent waves in each porous media, namely

$$\begin{cases} \phi_1^{(j)}(x,z,t) = p_{u1}^{(j)} e^{i(\omega t - \gamma_1^{(j)} z - kx)} + p_{d1}^{(j)} e^{i(\omega t + \gamma_1^{(j)} z - kx)}, \\ \phi_2^{(j)}(x,z,t) = p_{u2}^{(j)} e^{i(\omega t - \gamma_2^{(j)} z - kx)} + p_{d2}^{(j)} e^{i(\omega t + \gamma_2^{(j)} z - kx)}, \\ \psi^{(j)}(x,z,t) = s_u^{(j)} e^{i(\omega t - \nu^{(j)} z - kx)} + s_d^{(j)} e^{i(\omega t + \nu^{(j)} z - kx)}, \end{cases} \quad \textit{for } j = 1,2 . \qquad (1)$$

Substituting the above potentials into following boundary conditions at interface (z=0),

(1) Continuity of total displacement (normal & shear components),
(2) Continuity of total traction (normal & shear components),
(3) Continuity of the pressure of pore fluid,
(4) Continuity of fluid motion (normal component of fluid displacement),

we obtain,

$$\mathbf{D}_{11}^{(1)}\mathbf{c}_u^{(1)} + \mathbf{D}_{12}^{(1)}\mathbf{c}_d^{(1)} = \mathbf{D}_{11}^{(2)}\mathbf{c}_u^{(2)} + \mathbf{D}_{12}^{(2)}\mathbf{c}_d^{(2)}, \qquad (2a)$$

and

$$\mathbf{D}_{21}^{(1)}\mathbf{c}_u^{(1)} + \mathbf{D}_{22}^{(1)}\mathbf{c}_d^{(1)} = \mathbf{D}_{21}^{(2)}\mathbf{c}_u^{(2)} + \mathbf{D}_{22}^{(2)}\mathbf{c}_d^{(2)}, \qquad (2b)$$

where, $\mathbf{c}_u^{(j)} = [p_{u1}^{(j)}, p_{u1}^{(j)}, s_u^{(j)}]^T$ and $\mathbf{c}_d^{(j)} = [p_{d1}^{(j)}, p_{d1}^{(j)}, s_d^{(j)}]^T$ (j=1,2) are coefficient vectors for up-going and down-going waves, and $\{\mathbf{D}_{mn}^{(j)},\ n,m = 1,2;\ j = 1,2\}$ are 3 by 3 matrices whose explicit expressions are given in Appendix.

The reflection and transmission coefficients are defined by the following relations,

$$\begin{cases} \mathbf{c}_u^{(1)} = \mathbf{R}_{du}\mathbf{c}_d^{(1)} + \mathbf{T}_u\mathbf{c}_u^{(2)} \\ \mathbf{c}_d^{(2)} = \mathbf{T}_d\mathbf{c}_d^{(1)} + \mathbf{R}_{ud}\mathbf{c}_u^{(2)} \end{cases}, \qquad (3)$$

where, $\mathbf{R}_{du}$, $\mathbf{T}_u$, $\mathbf{T}_d$ and $\mathbf{R}_{ud}$ are all 3 by 3 matrices which have the following form

$$\mathbf{X} = \begin{bmatrix} X^{P_1P_1} & X^{P_1P_2} & X^{P_1S} \\ X^{P_2P_1} & X^{P_2P_2} & X^{P_2S} \\ X^{SP_1} & X^{SP_2} & X^{SS} \end{bmatrix}. \qquad (4)$$

By comparing equation (2) with (3) we can obtain the following exact expression of reflection and transmission coefficients in porous media,

$$\begin{bmatrix} \mathbf{R}_{du} & \mathbf{T}_u \\ \mathbf{T}_d & \mathbf{R}_{ud} \end{bmatrix} = \begin{bmatrix} \mathbf{D}_{11}^{(1)} & -\mathbf{D}_{12}^{(2)} \\ \mathbf{D}_{21}^{(1)} & -\mathbf{D}_{22}^{(2)} \end{bmatrix}^{-1} \begin{bmatrix} \mathbf{D}_{11}^{(2)} & -\mathbf{D}_{12}^{(1)} \\ \mathbf{D}_{21}^{(2)} & -\mathbf{D}_{22}^{(1)} \end{bmatrix}. \qquad (5)$$

NUMERICAL EXAMPLES

Let us first compare the our exact solution with effective elastic P-P (precisely speaking, should be fast P to fast P) reflection coefficients for Biot model for water, oil and gas saturated porous media, respectively. The upper and lower media are shale and sandstone, whose elastic and porous parameters are $\rho_s^{(1)}$=2.6774 g/cm^3, $\alpha_s^{(1)}$ =4.7877 km/s, $\beta_s^{(1)}$=2.52 km/s, $\phi^{(1)}$=0.16, $\kappa^{(1)}$=0.0014 md, and $\rho_a^{(1)}$ =0.38 g/cm^3 for shale, and $\rho_s^{(2)}$=2.6284 g/cm^3, $\alpha_s^{(2)}$ =5.4497 km/s, $\beta_s^{(2)}$=3.2438 km/s, $\phi^{(2)}$=0.19, $\kappa^{(2)}$=100 md, and $\rho_a^{(2)}$=0.42 g/cm^3 for sandstone. The properties of pore fluids are ρ_{water} =1.0 g/cm^3, ρ_{gas} =0.14 g/cm^3, ρ_{oil}=0.88 g/cm^3, η_{water}=1.0 cp, η_{gas}=0.022 cp and η_{oil}=180 cp. The comparisons for f=100 Hz shown in Figure 2 are for water, oil and gas saturated cases, respectively. Here, the solid lines stand for the exact solutions and dashed lines for effective elastic ones. We find that for this frequency our exact solutions agree excellently with the effective elastic ones. Figure 3 shows the comparisons of reflection with vertical incidence (i.e., θ=0) in the frequency range of 1Hz to 10^8Hz, and the corresponding distributions of *effective* elastic velocities of P wave (fast P wave) and S wave in the same frequency range. We can see that the departure of the effective elastic solution from the exact one in porous media occurs from the Biot's critical frequency.

Using our exact reflection coefficient formula of porous media, we can directly relate the reflection coefficient to the porous parameters (e.g., porosity, permeability, fluid density and viscosity, etc.). Figure 4 shows the distributions of reflection coefficients with vertical incidence (θ=0) for various porosities and permeabilities, respectively.

As shown in Figure 1(b) those phase velocities of BISQ model depart from those of Biot model at low frequency limit, and converge to same value at high frequency limit. Therefore, we expect that the resulting reflection coefficients of BISQ model will be different from those of Biot model at low frequency, and become same as those of Biot model at high frequency limit. Since the AVO analysis is a low frequency problem, the discrepancy of phase velocities between Biot and BISQ models will lead to the difference of reflection coefficients between these two models, consequently will affect the AVO analysis. We could also directly relate the reflection coefficient of BISQ model to the porous parameters of the saturated porous media, but our computer code doses not run through yet at this moment, and we are still working on this problem.

DISCUSSIONS AND CONCLUSIONS

We have rigorously derived an exact formula for computing the reflection and transmission coefficients in porous media, and verified its validity by comparing with the effective elastic solution (i.e., conventional solution). Using this exact formula we can directly relate the reflection coefficients to the parameters of porous media, such as porosity, permeability, fluid density and viscosity, etc.). Therefore, this new exact solution of porous media may be useful for AVO analysis. The BISQ model (Dvorkin and Nur, 1993), on the other hand, gives rise to notably smaller phase velocities at low frequency, thus it will give notably different reflection coefficients. Consequently, it will be significantly affect the results of AVO analysis.

According to our numerical results shown above, we find that at high frequency ($f > f_c$) the effective elastic solution departs from the exact solution of porous media. Thus, in well-logging analysis where the characteristic frequency is near the Biot's critical frequency, we need to use the exact solution of porous media rather than the effective elastic solution. Next, we shall apply our rigorous method to the study of full waveform logging in radially layered media.

REFERENCES

Biot, M. A., 1956a, Theory of propagation of elastic waves in a fluid-saturated porous solid. I. Low-frequency range: J. Acoust. Soc. Am., **28**, 168-178.

Biot, M. A., 1956a, Theory of propagation of elastic waves in a fluid-saturated porous solid. II. Higher-frequency range: J. Acoust. Soc. Am., **28**, 179-191.

Biot, M. A., 1962a, Mechanics of deformation and acoustic propagation in porous media: J. Appl. Phys., **33**, 1482-1498.

Biot, M. A., 1962b, Generalized theory of acoustic propagation in porous dissipative media: J. Acoust. Soc. Am., **34**, 1254-1264.

Dvorkin, J. and Nur, A., 1993, Dynamic poroelasticity: a unified model with the squirt and Biot mechanism, Geophysics, **58**, 524-533.

Paillet, F. L. and Cheng, C. H., 1993, *Acoustic waves in boreholes*, CRC Press.

Schmitt, D. P. , Bouchon, M. and Bonnet, G., 1988, Full-waveform synthetic acoustic logs in radially semi-infinite saturated porous media, Geophysics, **53**, 807-823.

APPENDIX

Those 3x3 matrices in equation (2), $\{\mathbf{D}^{(j)}_{mn},\ n,m=1,2;\ j=1,2\}$, are defined as,

$$\mathbf{D}^{(j)}_{nm}=\begin{bmatrix} a^{(j)}_{3(n-1)+1,3(m-1)+1} & a^{(j)}_{3(n-1)+1,3(m-1)+2} & a^{(j)}_{3(n-1)+1,3(m-1)+3} \\ a^{(j)}_{3(n-1)+2,3(m-1)+1} & a^{(j)}_{3(n-1)+2,3(m-1)+2} & a^{(j)}_{3(n-1)+2,3(m-1)+3} \\ a^{(j)}_{3(n-1)+3,3(m-1)+1} & a^{(j)}_{3(n-1)+3,3(m-1)+2} & a^{(j)}_{3(n-1)+3,3(m-1)+3} \end{bmatrix} \quad \text{for } j=1,2,$$

where,

$$a^{(j)}_{11}=a^{(j)}_{14}=\alpha^{(j)}_{1}k,$$

$$a^{(j)}_{12}=a^{(j)}_{15}=\alpha^{(j)}_{2}k,$$

$$a^{(j)}_{13}=-a^{(j)}_{16}=\alpha^{(j)}_{3}v^{(j)},$$

$$a^{(j)}_{21}=-a^{(j)}_{24}=-\alpha^{(j)}_{1}\gamma^{(j)}_{1},$$

$$a^{(j)}_{22}=-a^{(j)}_{25}=-\alpha^{(j)}_{2}\gamma^{(j)}_{2},$$

$$a_{23}^{(j)} = a_{26}^{(j)} = \alpha_3^{(j)} k,$$

$$a_{31}^{(j)} = -a_{34}^{(j)} = 2\gamma_1^{(j)} N^{(j)} k,$$

$$a_{32}^{(j)} = -a_{35}^{(j)} = 2\gamma_2^{(j)} N^{(j)} k,$$

$$a_{33}^{(j)} = -a_{36}^{(j)} = \alpha_3^{(j)} N^{(j)} [(v^{(j)})^2 - k^2],$$

$$a_{41}^{(j)} = a_{44}^{(j)} = -\{2N^{(j)}(\gamma_1^{(j)})^2 + [F^{(j)} + G^{(j)} + (T^{(j)} + G^{(j)})C_1^{(j)}](k_{p1}^{(j)})^2\},$$

$$a_{42}^{(j)} = a_{45}^{(j)} = -\{2N^{(j)}(\gamma_2^{(j)})^2 + [F^{(j)} + G^{(j)} + (T^{(j)} + G^{(j)})C_2^{(j)}](k_{p2}^{(j)})^2\},$$

$$a_{43}^{(j)} = -a_{46}^{(j)} = 2k\alpha_3^{(j)} N^{(j)} v^{(j)},$$

$$a_{51}^{(j)} = a_{54}^{(j)} = -(G^{(j)} + T^{(j)} C_1^{(j)})(k_{p1}^{(j)})^2 / \phi^{(j)},$$

$$a_{52}^{(j)} = a_{55}^{(j)} = -(G^{(j)} + T^{(j)} C_2^{(j)})(k_{p2}^{(j)})^2 / \phi^{(j)},$$

$$a_{53}^{(j)} = a_{56}^{(j)} = 0,$$

$$a_{61}^{(j)} = -a_{64}^{(j)} = -C_1^{(j)} \gamma_1^{(j)},$$

$$a_{62}^{(j)} = -a_{65}^{(j)} = -C_2^{(j)} \gamma_2^{(j)},$$

$$a_{63}^{(j)} = a_{66}^{(j)} = \chi^{(j)} k,$$

$$\alpha_{1,2}^{(j)} = 1 - \phi^{(j)} + \phi^{(j)} C_{1,2}^{(j)},$$

$$\alpha_3^{(j)} = 1 - \phi^{(j)} + \phi^{(j)} \chi^{(j)},$$

$$v^{(j)} = \sqrt{(k_s^{(j)})^2 - k^2},$$

$$\gamma_{1,2}^{(j)} = \sqrt{(k_{p1,2}^{(j)})^2 - k^2},$$

$$k_{p1,2}^{(j)} = \omega / V_{p1,2}^{(j)},$$

and

$$k_s^{(j)} = \omega / V_s^{(j)}.$$

Where, the $C_{1,2}^{(j)}$, $\chi^{(j)}$, $F^{(j)}$, $N^{(j)}$, $G^{(j)}$ and $T^{(j)}$ have same definitions as those in Paillet and Cheng (1993).

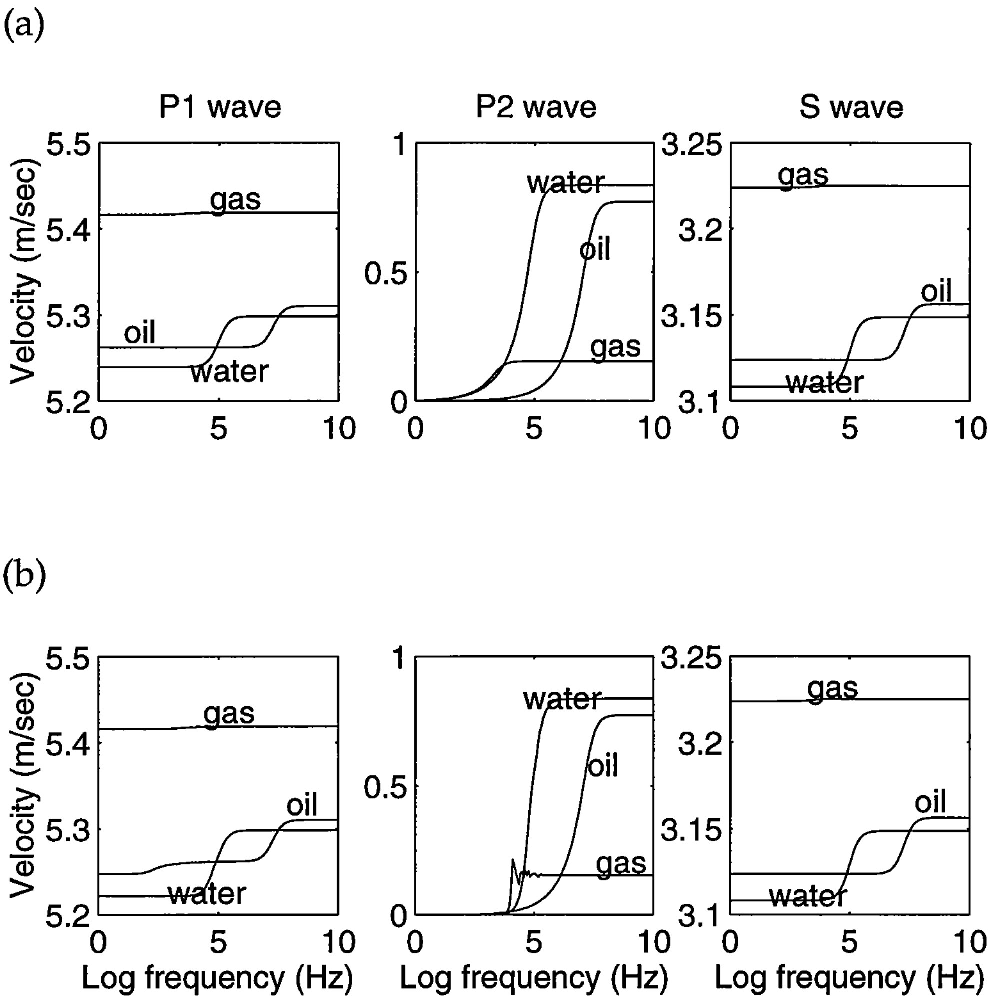

Figure 1. Phase velocities for saturated sandstone. (a) Phase velocities of Biot model; (b) phase velocities of BISQ model (Dvorkin and Nur, 1993).

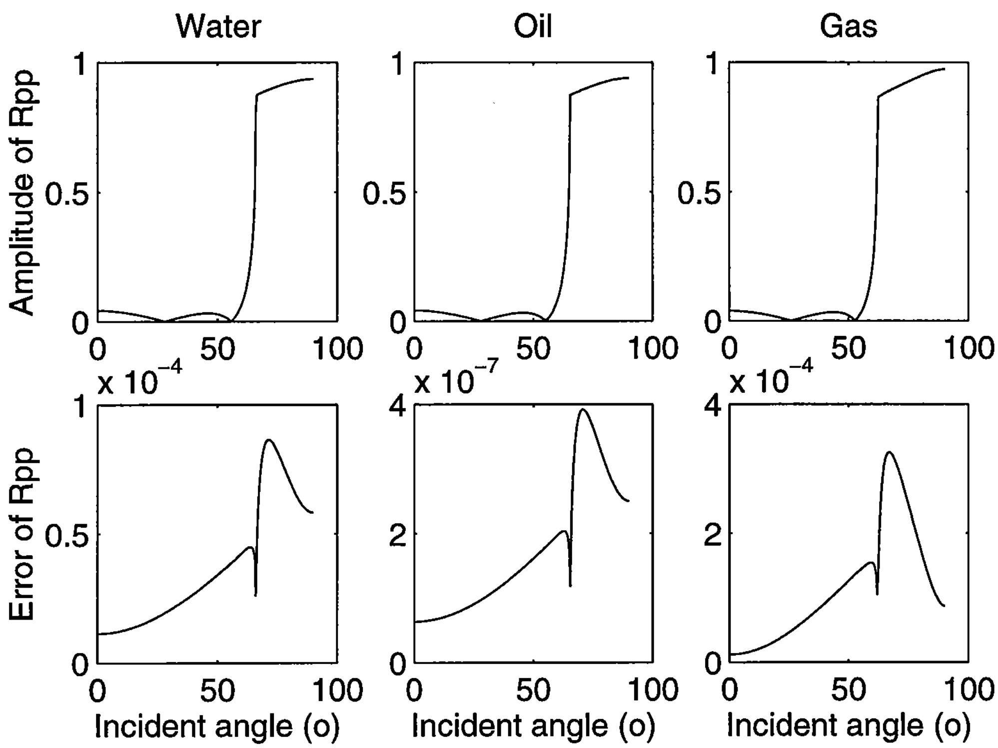

Figure 2. Comparisons of reflection coefficients of porous media between the exact solutions (solid lines) and effective elastic solutions (dashed lines) for different pore fluids. Here f=100 Hz.

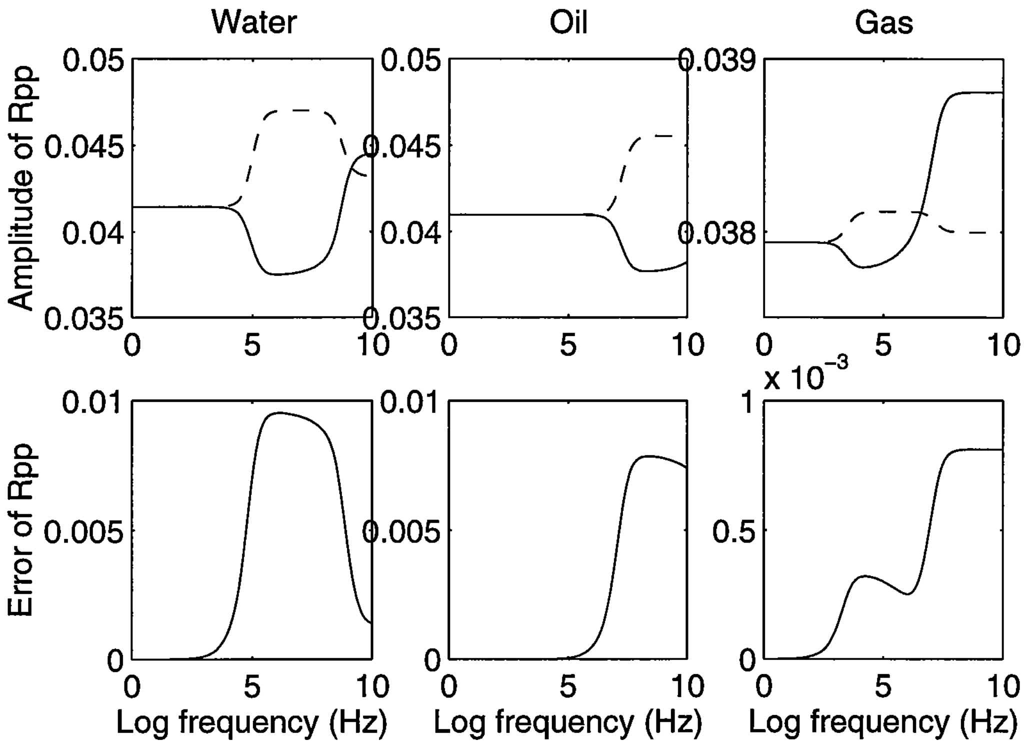

Figure 3. Comparisons of exact solutions (solid lines) with effective elastic solution of vertical incidence over a frequency range from 1Hz to 10^{10} Hz.

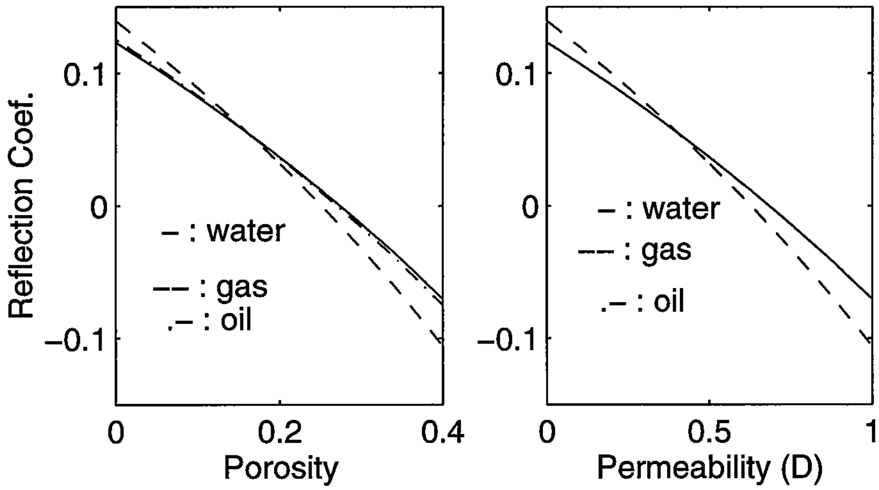

Figure 4. Relationships of reflection coefficients with the porosity and permeability. Where, the solid, dashed and dot-dashed lines denote, respectively, the water, gas and oil saturated porous media.